Main Manuscript for

Analgesia through FKBP51 inhibition at disease onset confers lasting relief from sensory and emotional chronic pain symptoms

Sara Hestehave[1,2], Roxana Florea[1], Samuel Singleton[3], Alexander J.H. Fedorec[1], Sara Caxaria[4], Oakley Morgan[1], Katharina Tatjana Kopp[5], Laurence A. Brown[6], Tim Heymann[7], Shafaq Sikandar[4], Felix Hausch[7,8], Stuart N. Peirson[9], Sandrine M. Géranton[1*].

[1]Dept. of Cell & Developmental Biology, University College London, WC1E 6BT, United Kingdom.
[2]Current address; Dept. Of Veterinary and Animal Sciences, University of Copenhagen, 2000 Frederiksberg, Denmark.
[3] School of Medicine, University of Dundee, DD2 1UB, United Kingdom
[4]William Harvey Research Institute, Barts and The London School of Medicine and Dentistry, Queen Mary University, EC1M 6BQ, United Kingdom
[5]Department of Pharmacy, Pharmaceutical Technology and Biopharmaceutics, Ludwig-Maximilians-Universität München, Munich, 81377, Germany.
[6]Research IT, University of Oxford, OX1 2JD, United Kingdom
[7]Institute of Organic Chemistry and Biochemistry, Technical University Darmstadt, Darmstadt, 64287, Germany.
[8] Centre for Synthetic Biology, Technical University Darmstadt, Darmstadt, 64287, Germany
[9]Nuffield Department of Clinical Neuroscience, University of Oxford, OX3 9DU, United Kingdom.

***Correspondence to:** Sandrine M. Géranton; Medawar Building, Dept. of Cell & Developmental Biology, University College London, WC1E 6BT, United Kingdom; Tel: +442036793386.

Email: sandrine.geranton@ucl.ac.uk

Author Contributions: Study conception and experimental designs: SH SG. Data collection: SH, RF, SG, SC; TH synthesised SAFit2. KK prepared the VPG. Data analysis and interpretation: SH, SG SSingleton, AF. Manuscript preparation: SH, SSingleton and SG wrote the initial draft of the manuscript. All authors read and approved the final manuscript.

Competing Interest Statement: No competing interests exist.

Keywords: Chronic pain, stress, emotional comorbidities, FKPB51, SAFit2

Abstract

Chronic pain affects 20-30% of the population and imposes a significant socio-economic burden as it is often accompanied by substantial emotional comorbidities such as anxiety and depression. Yet, the mechanisms underlying the interactions between the sensory and emotional aspects of chronic pain remain poorly understood. Here, we investigated the role of FKBP51, a regulator of the stress response, in mediating both sensory and emotional symptoms of chronic pain. Inhibition of FKBP51, *via* genetic deletion or pharmacological blockade, in persistent joint pain reduced fast-onset sensory, functional and activity-related symptoms, as well as late anxio-depressive comorbidities. FKBP51 inhibition after the establishment of the hypersensitive state provided only temporary symptoms relief, while acute inhibition at disease onset protected from the full development of sensory and anxio-depressive symptoms for up to 6 months. Our results also indicated that early pain symptoms could predict the late sensory and emotional outcomes of chronic pain. RNA sequencing of spinal cord tissue revealed that late FKBP51 inhibition transiently altered nociceptive genes associated with mechanical hypersensitivity. In contrast, early inhibition persistently downregulated the *Naaa* gene, a key regulator of the transition to chronic pain, and reorganized spinal cilia. Our results indicate that early FKBP51 inhibition after injury can persistently reduce chronic pain and prevent the onset of associated emotional comorbidities by modulating critical spinal neurobiological pathways that play pivotal roles in the transition to chronic pain.

Significance statement

Our study reveals that early inhibition of FKBP51, a modulator in the stress axis, at the onset of joint damage provides sustained pain relief and significantly delays or prevents emotional comorbidities in a sex-dependent manner. In contrast, FKBP51 inhibition initiated after chronic pain is established results in only temporary symptoms improvement. These findings highlight a critical therapeutic window during which timely intervention can prevent the transition from acute to chronic pain. By establishing a predictive link between early therapeutic response and long-term outcomes, this work has important clinical implications for proactive and personalized chronic pain management.

62 **Main text**

63 **Introduction**

64 Despite recent advances in our understanding of the mammalian brain circuits that contribute
65 to the different aspects of pain, our knowledge of the neurobiology of chronic pain is still limited
66 and we are still seeking effective therapies that would improve patients' quality of life. Patients
67 with chronic pain often reports negative affective symptoms such as anxiety, depression and
68 disrupted sleep (1–3) but we still do not understand how these emotional comorbidities may be
69 mechanistically linked to the sensory outcomes of persistent pain. Improved understanding of
70 the interactions between the circuits that drive the emotional and the sensory components of
71 chronic pain may therefore shed further light on the mechanisms of pain chronicity.

72 In this context, FKBP51, a protein known to be involved in stress-modulation, was recently
73 highlighted as a crucial driver of chronic pain in rodents, where it acts at the level of spinal pain
74 circuits - known to generate widespread pain in chronic pain states - in a glucocorticoid
75 dependent manner (4–6). Genetic variations in *FKBP5,* the gene encoding for FKBP51,
76 influence the severity of musculoskeletal pain symptoms experienced by humans after trauma,
77 suggesting a universal role for FKBP51 in chronic pain (7–9). FKBP51 regulates the stress
78 response through modulation of the glucocorticoid receptor sensitivity. High levels of FKBP51
79 protein tend to be associated with a hyper-reactive stress pathway, as seen in patients with
80 depression, while low levels of FKBP51 dampen down the stress pathway and produce a more
81 robust and resilient individual (10). Supporting these observations, deletion of FKBP51 in
82 healthy mice has been shown to reduce anxiety-related behaviour (11, 12) and improve sleep
83 quality (13). Altogether, these observations suggest that blocking FKBP51 in chronic pain states
84 could modulate many emotional-related symptoms. Therefore, following our previous success
85 with FKBP51-manipulation to reduce hypersensitivity in persistent pain states (4, 5), our
86 hypothesis was that targeting the protein FKBP51 modulates sensory, functional and emotional
87 symptoms associated with chronic pain. Moreover, we have recently demonstrated that
88 hypersensitivity in the early stage of persistent pain can predict the intensity of later emotional
89 comorbidities (14). Therefore, we also anticipated that early FKBP51 inhibition would have long-
90 term implications on emotional comorbidities.

91 We have developed the first selective antagonists of FKBP51 described so far (15). Acute
92 administration of these antagonists recapitulates the anxiolytic properties of FKBP51 deletion
93 in mice (11). We have previously tested pre-clinically one of these compounds, SAFit2, and
94 found its administration at spinal cord level relieved hypersensitivity associated with persistent
95 pain states to the same extend as global deletion of *Fkbp5* and intrathecal delivery of siRNA
96 against *Fkbp5* (4, 5). Here, we use genetic and pharmacological blockade of FKBP51 in a
97 robust pre-clinical model of persistent joint pain, the MIA model (14), that induces sensory and
98 emotional symptoms, as experienced by chronic pain patients. We report that FKBP51
99 inhibition improves both the sensory and emotional component of persistent pain in a time

dependent manner. Crucially, acute FKBP51 inhibition at disease onset provided permanent relief of both pain and emotional symptoms and dampened the expression of *Naaa*, a crucial driver of the transition from acute to chronic pain.

Results

Study design and all statistical tests and full analysis results are presented in **SI Appendix Table S1, S2 andS3,** with statistically significant results summarized in the main manuscript and figures.

MIA caused immediate changes in sensory and functional outcomes and daily activity rhythms but had a delayed impact on the open field and sucrose preference test

We first established the complete behavioural characterisation of male and female mice with joint pain induced by the injection of monoiodoacetate (MIA) in the knee joint, for up to 6 months. Mechanical allodynia, assessed by application of manual von Frey filaments, rapidly developed in both sexes and was maintained throughout the 6-month period (Fig.1A1,2), with no obvious sex differences ('sex' effect Fig.1A2, P=0.0632). Both males and females also showed immediate and robust changes in weight bearing, with the greatest impairment in the first 3 weeks and a more pronounced effect in females (Fig.1B1,2). We also looked at bone volume, as a surrogate measure of bone deformation, and found that the injection of MIA had led to a full remodelling of the joint by 6 months, across sexes (Fig.1C1,2).

Looking at the affective aspect of the pain experience, we found no difference in stress hormone levels between injured and control mice, either at 48h or 30 days after MIA injection, suggesting that stress-hormone increase, if any, would have been short-lived (Fig.S1A). However, the duration of affective-motivational response to von Frey stimulation was promoted by MIA, especially in the first 3 weeks after injection, with a greater impact in females, as demonstrated by significant interactions between sex and injury (Fig. S1B1,2, C1,2 and D1,2). This outcome measure was more variable than mechanical thresholds, likely due to its greater complexity thought to be driven by higher-order cognitive, emotional, and environmental factors (16, 17). Since most animals had returned to baseline for this specific behavioural assessment by 6 weeks, it was discontinued at that point to reduce burden on the animals. Overall, these results suggested that the sensory impact of the MIA injection was almost immediately stable, while the functional and affective impairments peaked during the first 3 weeks of the disease state.

We next found that both male and female mice had reduced preference for sucrose from day 90 and this lasted for at least 6 months (Fig.1D1,2), suggesting depressive-like behavior. We had previously reported that reduced preference for sucrose is not universal among animals with chronic joint pain, much like depressive symptoms in chronic pain patients (14). Using an individual profiling approach, where affected animals are defined as responding one standard deviation or more from the average performance of the control group (14, 18, 19), we found that up to 75% of male mice showed reduced sucrose preference at 4 months, while 100% of

137 females exhibited this symptom by 6 months (Table S4). Moreover, both male and female mice
138 showed reduced exploration time of the middle of the arena in the OFT, suggesting anxiety-like
139 behaviour, from 3 months (27% of males and 45% of females, estimated by individual profiling,
140 Table S4), with no obvious sex differences (Fig.1E1-3). Interestingly, both sucrose preference
141 and time of exploration of the centre of the arena correlated with mechanical allodynia at 3 and
142 6 months across sexes (Fig.1F1,2). Furthermore, in line with our previous work establishing
143 that early pain-related burden may serve as a predictor of later disease outcome (14), we also
144 found that the early mechanical allodynia significantly correlated with sucrose preference and
145 mechanical allodynia at 3 and 6 months (Fig.1G1, 1G2, and Table S5). Time of exploration in
146 the centre of the arena was only significantly correlated to early allodynia at 3months, while
147 trending at 6months (Fig.S1E and Table S5 for all prediction correlations).

148 Finally, we characterised the activity patterns of single housed mice using non-invasive motion
149 sensor readouts validated against EEG (14, 20–22). Daily activity rhythms were no different
150 between 8-week-old naïve male and female mice (Fig.2A,B; Fig.S2), but were significantly
151 impacted by MIA in the early stages of the joint pain state, specifically during ZT14 and ZT1,
152 where mice would normally be active. There was a significant increase in the proportion of time
153 spent immobile, or in a sleep-like state, in that period, along with a significant reduction in
154 activity in both male and female mice (Fig.2C,D). There was a noticeable sex-effect, as injured
155 females could maintain activity levels for longer than injured male mice (Fig.2C,D, ZT14 to ZT1:
156 significant time x injury x sex interactions; Table S2). Summary statistics of circadian rhythm
157 confirmed these observations and indicated that injured mice were less able to sustain long
158 bouts of activity (Fig.2E1) and had increased immobility in the dark-phase (Fig.2E2) and
159 decreased immobility in light-phase (Fig.2E3). The impact of MIA on home-cage behaviour was
160 short-lasted, as previously reported for other pre-clinical models of persistent pain (23), and,
161 from one-month post injury, MIA-induced changes were subtle, while sex differences became
162 more obvious as mice aged (Fig.S3, S4).

163 ***Fkbp5* global deletion reduced MIA-induced sensory, functional and depressive-like**
164 **symptoms.**

165 We next asked whether the inhibition of FKBP51 could reduce the pain phenotype beyond its
166 documented effects on mechanical hypersensitivity (4–6, 24). First, we used *Fkbp5* global KO
167 mice (4, 5). Both male and female *Fkbp5* KO displayed MIA-induced mechanical allodynia and
168 weight bearing deficit that lasted for 6 months but was substantially reduced compared with
169 control WT littermates (Fig.3A1,2; B1,2). There were no sex*genotype-interaction affecting the
170 sensory and functional outcomes, suggesting that the *Fkbp5* deletion did not affect the two
171 sexes differently. However, as observed in Fig.1, females displayed higher functional deficits
172 across genotype, resulting in a sex-effect in the overall statistical analysis for this dataset (Table
173 S2). Importantly, *Fkbp5* deletion had no impact on MIA-induced bone deformation after
174 correction for body weight, important due to the leaner phenotype of the KO mice (25, 26)
175 (Fig.3C, Fig.S5A1,2; B). We also observed that *Fkbp5* knock-down mitigated the MIA-induced

176 decrease in sucrose preference across sexes, as up to 55.6% and 44.4% of males and females
177 KO mice respectively displayed a resilient phenotype (Fig.3D1,2, Table S6). *Fkbp5* deletion
178 had a milder impact on time of exploration in the centre of the OFT arena (Fig.3E, Table S6).
179 While these results might have been confounded by increased locomotion in the KO mice
180 (Fig.S5C), they were confirmed by EPM (Fig.S5D). Overall, there was no significant correlation
181 across sex and genotype between sensory and emotional outcomes, when compared at any
182 given time point (Fig.3F1,2). Moreover, while early mechanical allodynia was a significant
183 predictor of late pain sensitivity (Fig.3G1), it could not predict sucrose preference and time of
184 exploration of the centre of the arena at 3 or 6 months (Table S5, Fig 3G2,3). These results
185 suggested that *Fkbp5* global knockdown disrupted the relationship between pain burden and
186 emotional comorbidities, likely due to the reported impact of *Fkbp5* deletion on anxiety- and
187 depressive-like behaviour independently from the hypersensitive state (26–28).

188 We also characterised the impact of *Fkbp5* knockdown on daily activity rhythms. While there
189 were no obvious sex and genotype differences in 8-week-old naive mice (Fig.S6A, B, S7),
190 *Fkbp5* KO male and female mice showed increased activity between ZT14 and ZT1 after MIA,
191 when compared with WT mice (Fig.S6C,D). These results suggested that the deletion of *Fkbp5*
192 provided some protection from the injury-induced disruption to daily activity rhythms. Moreover,
193 MIA-induced disruption in a number of summary statistics of circadian parameters (Fig.2E)
194 were resolved by *Fkbp5* knockdown, including in long-bouts of activity (Fig.S6F). As mice aged
195 and at a time where the effects of the injury were no longer obvious in WT mice, genotype and
196 sex differences grew stronger (Fig.S6). In particular, the KO females were more active in the
197 dark phase and less immobile in the light phase than their wild–type counterparts (Fig.S8, S9).
198 Overall, these results suggested that the impact of global *Fkbp5* knockdown on immobility and
199 activity patterns went beyond the protection from MIA-induced disruptions.

200 **Pharmacological inhibition of FKPB51 after establishment of persistent pain provided**
201 **temporary improvement of sensory, functional and depressive-like symptoms.**

202 We next asked whether pain relief could be achieved through pharmacological blockade of the
203 protein FKBP51 using the FKBP51 inhibitor, SAFit2 (4, 5). SAFit2-VPG, a formulation designed
204 for the sustained released of the inhibitor over 7 days via encapsulation in a vesicular
205 phospholipid gel (VPG), was first administered 2 weeks after the MIA injection, a time point
206 when SAFit2 had been tested in models of ankle joint inflammation and neuropathic pain (4).
207 SAFit2-VPG attenuated the MIA-induced allodynia, with mechanical thresholds nearly returning
208 to baseline (Fig.S10A). Weight bearing deficit were equally improved (Fig.S10B). Next, we
209 delayed the administration of SAFit2-VPG to 1 month after MIA-induction, and, using weekly
210 injections, we extended the duration of FKBP51 inhibition to 3 weeks. SAFit2-VPG significantly
211 improved the MIA-induced mechanical allodynia (Fig.4A1,2) and weight bearing deficits
212 (Fig.4B1,2), during its controlled release from VPG, when it is therapeutically effective.

213 We next administered SAFit2-VPG for 4 weeks during the 2- to 3-month period after MIA
214 injection, when long-term emotional disorders manifest (Fig.1E, F). SAFit2-VPG improved
215 mechanical threshold and weight bearing deficit across sexes (Fig.4C1,2, D1,2) and delayed
216 the MIA-induced changes in sucrose preference (Fig.4E1,2), with up to 83.3% of males and
217 60% of females injected with SAFit2-VPG being resilient (Table S7). Unexpectedly, SAFit2-
218 VPG had no impact on the OFT exploration (Fig.4F, Fig.S10C-D, Table S7), nor did it affect
219 locomotor activity (Fig.S10E) or body weight (Fig.S10F). Furthermore, at 3 months, while
220 SAFit2 was still in its active release phase, there were significant correlations between
221 improvement of both functional and sensory outcome measures and the effect on sucrose
222 preference (Fig.4G). While mechanical thresholds quickly returned to control levels when the
223 treatment was discontinued, the effects on sucrose preference were maintained for longer, with
224 significant predictive correlations between the mechanical thresholds measured during the
225 active phase of SAFit2-treatment and the sucrose preference at 3, but not 6, weeks after
226 treatment-end (Fig.S10G,H; Table S5).

227 Surprised by the absence of effect of SAFit2-VPG on the OFT in injured mice, we explored the
228 effect of prolonged SAFit2-VPG in naïve mice. In a control experiment, SAFit2-VPG was
229 administered to naïve mice for one month. This reduced the time spent in the centre of the OFT
230 arena (Fig.S11A), which may explain its inability to prevent the MIA-induced reduction in centre
231 time. Finally, SAFit2 had no effect on mechanical threshold (Fig.S11B) or depressive-like
232 behaviour in naïve mice (Fig.S11C, D).

233 **Inhibition of FKBP51 at disease onset prevented the full development of MIA-induced**
234 **symptoms.**

235 We next explored the effect of early blockade of FKBP51 during the onset of the pain state and
236 observed a reduction in MIA-induced allodynia and both static and dynamic weight bearing
237 deficits (Fig.5A,B,C) of similar effect size as when SAFit2-VPG was given 2 weeks and 4 weeks
238 after MIA (Fig.S12A-F). Remarkably, for up to 6 months after injury, mechanical threshold and
239 weight bearing never reached the levels seen in vehicle treated MIA animals, despite SAFit2
240 being only active until day 14. The early SAFit2 treatment resulted in a sensory profile similar
241 to that of the *Fkbp5* KO mice. Importantly, early SAFit2 treatment did not exacerbate nor
242 prevented the degradation of the knee bone induced by MIA (Fig.S12G).

243 Early FKBP51 inhibition reduced affective responses to von Frey filaments (Fig.S13A, B, C)
244 and brush-induced allodynia (Fig.S13D) seen early after the initiation of the pain state. We also
245 found that the early treatment prevented the reduction in both sucrose preference and time
246 spent in the centre of the OFT arena (Fig.5D1,2, E, Fig.S13E) at 3 months after injury.
247 Specifically, the drop in sucrose preference in male mice was delayed until 6 months, with up
248 to 66.7% of male mice treated with SAFit2-VPG resilient at 3 months (Table S8). There was no
249 drop in sucrose preference in female mice, with up to 100% of female mice treated with SAFit2-
250 VPG resilient (Table S8). Finally, the early SAFit2-VPG administration did not lead to any

251 change in body weight compared with vehicle treated mice (Fig.S13F) and had no impact on
252 distance travelled in the OFT (Fig.S13G).

253 Pain-related outcomes (allodynia and weight bearing) showed the strongest correlations with
254 sucrose preference and exploration of the centre of the OF arena at 3 months across sexes,
255 weakening from 4.5 months (Fig.5F). SAFit2's early effects on pain-related measures predicted
256 late pain experience, as shown by correlations between early mechanical threshold and weight
257 bearing and late mechanical thresholds (Table S5), time spent in the centre of the OF arena
258 (Fig.5G1,2), and sucrose preference (Fig.5H1,2), with a predictive strength highest at 3 months
259 (Table S5).

260 Finally, SAFit2-VPG administered during the onset of the pain state had a protective effect on
261 the MIA-induced disruption to daily activity rhythms, as SAFit2-VPG-treated MIA mice slept less
262 and were more active than vehicle treated controls (Fig.5I,J). However, the impact of FKBP51
263 inhibition on summary parameters of activity rhythms were milder and rarely reached
264 significance (Fig.5K), and as mice aged, sex differences became more obvious (Fig.S14). As
265 we had observed an impact of SAFit2-VPG in the OFT in naïve mice, we also looked at activity
266 patterns in naïve mice treated with SAFit2-VPG and found an increase in activity in female and
267 a decrease in male mice during their active phase (ZT14 to ZT1, sex*treatment interactions;
268 Fig.S15A,B) but with no significant differences in the summary parameters of circadian
269 disruption (Fig.S15,C-N). Overall, the impact of early and acute FKBP51 pharmacological
270 inhibition on activity rhythms were milder than the global knock-down of *Fkbp5,* still improving
271 some of the MIA-induced deficits at peak burden.

272 **FKBP51 inhibition at disease onset downregulated genes involved in the transition to**
273 **chronic pain and reorganization of spinal cilia**

274 We used RNAseq to explore the mechanisms behind early *vs* late FKBP51 inhibition. Since
275 SAFit2 reduces pain sensitivity across all persistent pain states regardless of their origin, we
276 focused on comparing SAFit2 *vs* vehicle in MIA-injured mice, removing the confound of MIA.
277 One group received SAFit2-VPG or vehicle at pain onset (early), and another after pain was
278 established (late). As before, mice that received early SAFit2 treatment maintained mechanical
279 thresholds higher than controls beyond the compound's active phase (Fig.6A1,2). By day 30
280 post-MIA, mechanical thresholds were similar across all SAFit2-VPG treated mice. Early
281 treatment however yielded greater dynamic weight-bearing improvement (Fig.6B, S16A-D).
282 Corticosterone levels were reduced by SAFit2-VPG (Fig.6C) and correlated with the level of
283 allodynia (Fig.6D), supporting a functional relationship between FKBP51 activity, corticosterone
284 regulation and mechanical hypersensitivity, as previously reported (4, 5).

285 RNA sequencing of the ipsilateral dorsal horn quadrants aimed to identify differentially
286 expressed genes (DEGs) by SAFit2. We initially explored the main effect of treatment using
287 linear regression modelling of early and late SAFit2 groups compared with vehicle-treated
288 groups and detected 1185 DEGs (nominal $P<0.05$). Principal component analysis revealed

289 sub-clusters within the second principal component of SAFit2-VPG-treated groups exposed at
290 the early *vs* late time points absent in vehicle-treated groups, suggesting small time-dependent
291 regulation of gene expression by SAFit2 (Fig.6E). Out of the 1185 DEGs, 311 were up-
292 regulated and 534 were downregulated by SAFit2-VPG with a cut-off fold-change of 1.2 (Fig.6F,
293 total 845 DEGs). Notably, *Fkbp5* was one of the 311 up-regulated DEGs (Fig.6G).

294 To focus on pathways modified during the drug's active phase, we focused on the late treatment
295 group. A nested analysis ($Late_{SAFit2}$ *vs* $Late_{Vehicle}$) revealed 757 DEGs (adjusted FDR P<0.05,
296 cut-off fold-change of 1.2), with 425 upregulated and 332 downregulated genes (Fig.6H). We
297 next hypothesized that if the DEGs were functionally relevant to the reduced mechanical
298 threshold observed in $Late_{SAFit2}$ treated mice, their expression level would correlate with the
299 mechanical thresholds at time of dissection. Pearson's correlation analysis with Bonferroni
300 correction identified 702 DEGs that correlated with the mechanical threshold (average day 27
301 to day 30) but not with the guarding index (Fig.6B), suggesting that these genes were more
302 likely linked to the sensory rather than the functional aspect of the pain state. 434 of the 702
303 identified DEGs were not among the initial 1185 DEGs (Fig.6I), suggesting transient modulation
304 by SAFit2-VPG. Gene ontology (GO) analysis highlighted roles in energy metabolism, cell
305 structure regulation, neuronal development, RNA processing, protein transport and sensory
306 perception (Fig.S17). Downregulated DEGs linked to reduced hypersensitivity included
307 *Shank3,* linked to autism spectrum disorder and pain signalling (29, 30) (Fig.6J1). Conversely,
308 upregulated *Pten*, the gene encoding the Phosphatase and Tensin Homolog, may protect from
309 neuropathic pain (31) (Fig.6J2), while inhibition of the NF-KB inhibitor *Nfkbib* suggested
310 enhanced NF-KB signalling (Fig.6J3). However, some pain related genes were regulated in
311 ways potentially reinforcing hypersensitivity (Fig.S18).

312 We next investigated DEGs that were at the intersection of the 2 analyses (SAFit2 overall effect
313 - n=1185 and late treatment nested analysis - n=757: n=268 DEGs, Fig.6I). Of these, only one
314 (Eri1, involved in RNA metabolism) correlated with mechanical hypersensitivity when both
315 treatment groups were considered all together (Fig.6I). Several DEGs linked to nociceptive
316 signaling were also identified (Fig.S19), but their regulation alone could not explain the long-
317 term effects of early SAFit2 treatment, as late-treated animals were expected to return to full
318 hypersensitive state after the drug's active phase.

319 To uncover mechanisms of long-term pain relief driven by early SAFit2 treatment, we first drew
320 contrasts between $Early_{SAFit2}$ and $Early_{Vehicle}$ treated mice but found no DEGs with FDR-
321 corrected P<0.05. We then focused on the 1185 DEGs that were not modified by the late
322 treatment alone (*i.e.* 1185 Δ 757; n=893 DEGs; Fig.6I). GO analysis revealed that these 893
323 DEGs were mainly related to cilia motility and cytoskeleton organisation (Fig.S20). Further
324 analysis comparing the change in expression (SAFit2 Δ Vehicle) between early and late
325 treatments identified 202 annotated DEGs with greater modulation by early SAFit2 (Fig.6I).
326 While none of these genes correlated with mechanical thresholds, 32 of them correlated with
327 the guarding index which we found to be more strongly influenced by early SAFit2 treatment.

328 Many were associated with cilium-related processes (Fig.6K), while several genes previously
329 linked to pain phenotype (Fig.6L) were durably reduced by early SAFit2. These included the
330 preproenkephalin gene *Penk*, which encodes precursors to the endogenous opioid peptides
331 enkephalins, *Enkur,* which encodes the protein enkurin, known to interact with TRPC channels
332 and *Naaa*, which encodes the enzyme N-acylethanolamine acid amidase, and crucially had
333 been previously implicated in the transition from acute to chronic pain(32).

334 Altogether, our RNAseq analysis suggested early SAFit2 treatment induced lasting spinal cord
335 gene expression changes absent in late treatment, potentially driving sustained pain relief.
336 While FKBP51 is predominantly expressed in neurones in the rodent spinal cord (5), identified
337 DEGs were likely to be expressed in various cell types but changes reported here could not be
338 attributed to altered cell type composition (Fig.S21).

339 ## Discussion

340 Our study provides a comprehensive analysis of the behavioural and molecular impact of
341 FKBP51 inhibition in a persistent pain state (see Fig.S22: Summary of Findings). The MIA
342 model, which replicates key histological and functional alterations seen in osteoarthritis (OA),
343 allowed us to investigate both sensory and emotional dimensions of pain (33–39). MIA injection
344 rapidly produced a hypersensitive state lasting at least 6 months in male and female mice,
345 alongside progressive anxiety- and depressive-like behaviours. These emotional comorbidities
346 emerged in a subset of animals, as seen in chronic pain patients (40). This temporal
347 dissociation between immediate sensory changes and delayed emotional disturbances is
348 consistent with previous clinical and pre-clinical observations indicating a gradual onset of
349 emotional symptoms in chronic pain states (14, 40–45). Small but significant sex differences
350 were found in pain sensitivity and functional deficits, with females more affected by MIA, while
351 emotional comorbidities showed more complex sex effects.

352 Regardless of sex differences, both sensory and functional aspects of late-stage joint pain
353 correlated with emotional comorbidities across sexes, as seen in patients, where anxiety and
354 depression are positively associated with pain severity (45). More importantly, early sensory
355 and functional measures correlated with late pain intensity and depressive-like behaviours, as
356 we had previously observed in males (14). Further strengthening the idea that the early pain
357 burden could serve as a predictor of late emotional outcomes, FKBP51 inhibition during disease
358 onset not only permanently blunted MIA-induced allodynia, as observed in a trauma-induced
359 pain model (6), but also substantially reduced late anhedonia and anxiety-like behaviour. Since
360 pain behaviours in the MIA model peak early, this effect may have resulted indirectly from
361 reducing peak pain levels rather than from the timing of the intervention itself.

362 As many other pain management options, FKBP51 inhibition after the establishment of the pain
363 state (between 2 weeks and 2 months post-onset) provided transient benefit only, rather than
364 a long-lasting cure, likely through the modulation of central signalling pathways. Overall, our
365 results support our original hypothesis, that FKBP51 inhibition - which we previously showed
366 improves injury-induced mechanical hypersensitivity in a glucocorticoid-dependent manner (5)
367 - would alleviate both the sensory and emotional impact of persistent pain. When FKBP51
368 inhibition was provided at 2-3 months, just before the typical onset of comorbidities, it effectively
369 delayed depressive-like behaviour. This suggests that onset of depressive comorbidity in
370 chronic pain is likely to be secondary to sensory and functional effects, as reported by others
371 (46). It also suggests that the impact of FKBP51 inhibition on pain-induced depression is
372 secondary to pain improvement, supported by a significant correlation between the early pain
373 intensity and the later depressive comorbidity. Nonetheless, a direct effect of FKBP51 inhibition
374 on depressive-like behaviour cannot be excluded.

375 It is noteworthy that long-term FKBP51 blockade *(i.e.* for 4 weeks) in injured mice had no impact
376 on MIA-induced anxiety-like behaviour. This may not be surprising as long-term SAFit2

377 treatment alone in naïve mice caused anxiety-like behaviour, unlike the acute administration
378 that is known to have anxiolytic effects (11, 12). Any anxiolytic effects of SAFit2 resulting from
379 pain relief in injured mice may therefore have been counteracted by the anxiogenic effects
380 observed after long-term use. While SAFit2 never worsened anxiety-like behaviour in injured
381 mice, it may however have significant impacts on circadian patterns. Indeed, circadian
382 alterations outlasted the short-lived MIA-induced changes in the KO mice with no clear benefit
383 on immobility defined sleep. Nonetheless, FKBP51 has been identified as a target for stress-
384 induced sleep disorders, and its deletion promotes better sleep in disease states (13).
385 Importantly, acute SAFit2-VPG treatment at disease onset had no long-lasting impact on sleep-
386 like immobility and activity, suggesting stronger therapeutic potential for an early and acute
387 FKBP51 targeted pharmacotherapy.

388 Overall, acute pharmacological inhibition of FKBP51 at the onset of the disease provided
389 effective and long-lasting pain relief, which continued beyond the drug's active phase. To
390 elucidate the mechanisms underlying these observations, we investigated gene expression
391 changes induced by SAFit2 treatment given at the onset or during the maintenance phase of
392 the pain state in MIA mice, avoiding the confound of MIA-induced changes (for alternative
393 approach see Table S9). We focused on the spinal cord, specifically the ipsilateral quadrant of
394 the superficial dorsal horn, as our original work using spinal specific genetic and
395 pharmacological manipulations of *Fkbp5* suggested that FKBP51 drives chronic pain through
396 spinal mechanisms (5). While unlikely, as MIA injection into the knee joint does not increase
397 *Fkbp5* expression in DRGs (Fig.S23), the effect of systemic FKBP51 inhibition observed in our
398 study could nevertheless be secondary to changes in peripheral tissues.

399 Genes uniquely modified by active SAFit2, and therefore transiently modulated by FKBP51
400 inhibition, often correlated with mechanical hypersensitivity, suggesting some potential
401 functional relevance. These belonged to various biological processes including sensory
402 perception and a number had been previously involved with nociceptive signalling including
403 *Shank3 and Pten*. Surprisingly, we did not observe changes in glucocorticoid signalling, despite
404 SAFit2's impact on corticosterone levels. However, this effect was relatively mild, and previous
405 studies have also reported mild influence of SAFit2 on stress hormone levels (47). On the other
406 hand, we observed a decrease in *Nfkbib* expression, indicating that SAFit2 may promote NF-
407 κβ signalling. The role of FKBP51 in this context is complex, with previous studies suggesting
408 that it could both inhibit and facilitate NF-κβ signalling in various cell types (48).

409 While no genes were significantly modulated by early SAFit2 treatment alone (FDR $P<0.05$,
410 1.2-fold), we identified DEGs modulated by SAFit2 overall that were not significantly changed
411 by the late treatment. This suggested that the early treatment likely drove the differential
412 regulation. Most DEGs showing greater changes after early treatment were associated with
413 cilium movement and assembly. The primary cilium is a key organelle in cellular signaling,
414 present in most post-mitotic cells, including neurons in the CNS. While its role in spinal neurons
415 has been understudied, cilia-related genes have recently been linked to nociceptive signaling.

416 Primary cilia in both large and small neurons of the dorsal horn have been described (49) and
417 their role in Sonic Hedgehog (Shh) signaling, which modulates pain, has been highlighted in
418 nociceptors (50). Our findings suggest that long-term re-organisation of spinal cilia following
419 early SAFit2 treatment may provide long-term pain relief. Interestingly, it was recently
420 suggested that the μ- opioid receptor selectively localize to primary cilia in the mouse CNS (51),
421 which may contribute to the phenotype observed in early treated mice. We also found that early
422 SAFit2-VPG treatment persistently reduced the expression of *Penk*, the gene encoding for
423 preproenkephalin, while *Penk* derived peptides have been shown to delay recovery from
424 inflammatory hypersensitivity (52). Finally, one non cilium related DEG particularly stood out,
425 the *Naaa* gene which encodes the enzyme N-acylethanolamine acid amidase (NAAA). NAAA
426 has been identified as a crucial control point in the progression to pain chronicity and inhibition
427 of NAAA in the spinal cord after peripheral injury during a 72h time window can prevent chronic
428 pain (32). Here, we found that SAFit2-VPG treatment in a similar time window after MIA
429 injection led to a long-lasting downregulation of *Naaa* compared with controls and mice that
430 received SAFit2-VPG later.

431 Our study reveals key neurobiological mechanisms underlying the modulation of persistent pain
432 through FKBP51 inhibition, focusing on spinal circuits and molecular pathways. Early FKBP51
433 inhibition induced long-lasting changes in nociceptive signaling, including the downregulation
434 of *Naaa*, a gene pivotal in the transition to chronic pain, and reduced expression of *Penk*, which
435 encodes peptides delaying recovery from hypersensitivity. We identified genes associated with
436 cilia function and assembly, suggesting that primary cilia in spinal neurons may play a critical
437 role in pain modulation through pathways such as Sonic Hedgehog (Shh) signaling and possibly
438 μ-opioid receptor localization. These findings provide novel insights into the spinal mechanisms
439 governing the sensory and emotional dimensions of persistent pain, emphasizing the
440 importance of early molecular changes in shaping long-term pain outcomes.

441 Materials and Methods

442 Extended materials and methods can be found in SI Appendix.

443 ***Animals and housing;***

444 Male and female mice were used at 8-10 weeks of age, either C57Bl/6J, Charles River, UK or
445 *Fkbp5* KO colony, maintained in house (C57Bl/6J and Swiss Webster background). All
446 experiments comparing wild-type (WT) and knockout (KO) animals were performed using WT
447 and KO littermates bred in our colony. Mice were kept in groups of 2-4 in a temperature- and
448 light-controlled environment with *ad libitum* provision of food and water. Experiments were
449 conducted under the Home Office License P8F6ECC28 and ARRIVE guidelines were followed
450 for reporting.

451 ***Compound preparation and administration:***

452 SAFit2 was synthesised as before (15), encapsulated in Vesicular Phospholipid Gel (VPG) in
453 a dose of 10mg/ml. SAFit2-VPG was provided subcutaneously under anaesthesia in a dose of
454 1mg/10g, providing approximately 7 days of slow release (4). SAFit2 has a terminal plasma
455 half-life in mice of 9.7h, a rather high (15) volume of distribution, and moderate brain
456 permeability (53).

457 ***Study design;***

458 The study was divided in a series of experiments, each with different constellations of tests and
459 duration, designed to answer specific questions (Table S1). Key outcomes, including
460 mechanical sensitivity and weight bearing, were assessed frequently through most
461 experiments, while catwalk, activity, anxiety- and depressive-like behavior were only assessed
462 at selected time points, based on previous experience(14), the characterization study (Fig 1)
463 and hypothesis of each individual experiment.

464 ***Experimental procedures;***

465 *Induction of injury, (MIA);* Induction of the Monoiodoacetate Arthritis Model to the knee joint
466 (MIA) was performed under anaesthesia as previously reported(14, 35), injecting 1mg Sodium
467 Iodoacetate (Sigma) in 10µl saline in the left knee joint. Naïve control animals were only
468 exposed to anesthesia.

469 ***Behavioural testing;***

470 Behavioural testing was performed in randomized order by the same female experimenter, who
471 was blinded to treatment and/or genotype.

472 *Mechanical allodynia (VF);* low intensity mechanical sensitivity was assessed as previously
473 (14), using a series of calibrated von Frey monofilaments (Ugo Basile SRL, Italy). The 50%
474 response threshold was determined using the Dixon up-down method, using the following
475 equation; 50% threshold (g) = $10^{\log(\text{last filament})+k*0.3}$, where the response pattern determined the
476 constant, *k*(54).

477 *Affective-motivational behavior (AF);* We assess the affective responses displayed after
478 stimulation with selected filaments (low; 0.04g, medium; 0.16g, high; 1.0g as previously (14).
479 The duration of conscious attending behavior incl. licking, biting, lifting or guarding the paw,
480 was quantified within 30 seconds after stimulation.

481 *Functional impairment - Weight bearing (WB);* static weight bearing distribution across the two
482 hindlimbs was assessed as previously(14, 55), using the Bioseb Incapacitance Test (Bioseb),
483 and calculated as: WB-% = (weight borne on the injured leg/weight borne on both legs) * 100%.

484 *Catwalk gait analysis:* analysis of voluntary movement and dynamic gait pattern was performed
485 using the Catwalk® XT 10.0 system (Noldus Information Technology) as before (14, 42). For
486 outcome-measures like swing-time ratio, contact area and single stance, the data was
487 converted into a ratio between ipsi- and contra-lateral hind-limbs. The “guarding index” was

488 calculated as previously described (56) and the higher guarding index suggests less dynamic
489 weight bearing on the injured leg compared with the non-injured.

490 *Sucrose Preference Test (SPT);* the SPT was used to measure anhedonia, as before (14). The
491 preference for drinking water vs 1% sucrose was assessed in the home-cage environment for
492 12h overnight, during two nights with the sucrose bottle presented in the opposite side, to
493 account for potential side-preference, as reported previously (42). The sucrose preference %
494 was calculated across the two nights; SPT% = (sucrose-solution consumed / (total fluid
495 consumption)) * 100%.

496 *Elevated Plus Maze (EPM) and Open Field Test (OFT);* to assess anxiety-like behaviour,
497 animals were assessed during a 5min EPM- or OFT-test, as before (14, 42). Recording was
498 performed by a camera placed above the maze/arena, and movement between zones was
499 tracked using EthoVision XT14 (Noldus Information Technology). Anxiety-like behavior was
500 suggested by less time spent in the open arms (EPM) or center of the arena (OFT).

501 *Sleep-like/activity-pattern;* to measure undisturbed activity in the home-cages, we adopted the
502 approach of Brown et al. (14, 20) using non-invasive passive infrared motion sensors to record
503 single-housed animals every 10 seconds across multiple-day periods. As previously validated
504 against EEG-recording, immobility defined sleep, referred to as immobility in the manuscript,
505 was defined as periods in which no activity was measured for 40 seconds or more. Several
506 summary statistics of circadian disruption were calculated for individual animals across the 5-
507 to-14-day periods (depending on the experiment) and, where appropriate, on each individual
508 day: inter-daily stability, intra-daily variability, light-phase activity, dark-phase immobility, the
509 Lomb-Scargle periodogram, similar to the chi-square periodogram (20).

510 ***ELISA;***

511 Plasma corticosterone levels were quantified using a commercial ELISA kit for corticosterone
512 (Corticosterone ELISA kit, ab108821, Abcam PLC) according to the manufacturer's instructions
513 (4, 5).

514 ***Sequencing;***

515 RNA was extracted from lumbar (L4-L6) spinal cord and sequencing libraries prepared using
516 standard approaches outlined in SI Appendix. Next generation sequencing (NGS) was
517 performed for 150 cycles on a NextSeq®500 (Illumina) to generate 75 bp paired-end reads with
518 19.5M coverage on average per sample. Sequencing reads were aligned to mouse GRCm38
519 (mm10) reference genome. RNA transcripts exceeding a 1.2-fold change in expression and
520 Benjamini-Hochberg adjusted p-values < 0.05 were considered differentially expressed. We
521 additionally performed exploratory analysis on transcripts with p-values exceeding nominal (p
522 < 0.05) significance.

523 ***CT scans;***

524 Micro-CT analyses of knee joints were performed using VECTor6CT (MILabs, The
525 Netherlands), and analysed using BoneJ software for bone volume (BV) in region of interests
526 (ROI). Macroscopic analysis was done using VivoQuant version 4 software (Invicro LLC,
527 Boston, MA, USA).

528 ***Statistical analysis;***

529 Statistical tests were performed in IBM SPSS Statistic Program (vers 26) or GraphPad Prism
530 (vers 9). Interrogation of RNAseq data performed in R Studio version 4.3.3 or later. $P<0.05$ was
531 considered statistically significant. Individual animals were considered as experimental unit,
532 and sample-size was based on previous experience, based primarily on securing enough power
533 for the assessment of depressive-like behavior across sex. All statistical tests and significant
534 F-values are reported in SI Appendix Table S2 and S3, and key ANOVA-results are presented
535 in the figures. Tests for normality of residuals and homogeneity of sample variances was
536 confirmed before parametric analysis. The VF-dataset was log-transformed to ensure a normal
537 distribution(5, 57).

538 Acknowledgments

539 This project was funded by a Versus Arthritis grant to SG and FH; Research Award 21972.
540 SSingleton was funded by the Advanced Pain Discovery Platform (MR/W002566/1). SNP is
541 funded by the BBSRC (BB/X002357/1) and the NC3Rs (NC/V000977/1).

542 ## References

543 1. F. Radat, A. Margot-Duclot, N. Attal, Psychiatric co-morbidities in patients with chronic
544 peripheral neuropathic pain: A multicentre cohort study. *Eur. J. Pain* **17**, 1547–1557
545 (2013).

546 2. M. M. J. G. Gerrits, *et al.*, Impact of pain on the course of depressive and anxiety
547 disorders. *Pain* **153**, 429–436 (2012).

548 3. G. J. G. Asmundson, J. Katz, Understanding the co-occurrence of anxiety disorders and
549 chronic pain: state-of-the-art. *Depress. Anxiety* **26**, 888–901 (2009).

550 4. M. Maiarù, *et al.*, The stress regulator FKBP51: a novel and promising druggable target
551 for the treatment of persistent pain states across sexes. *Pain* **159**, 1224–1234 (2018).

552 5. M. Maiarù, *et al.*, The stress regulator FKBP51 drives chronic pain by modulating spinal
553 glucocorticoid signaling. *Sci. Transl. Med.* **8**, 325ra19 (2016).

554 6. B. J. Wanstrath, *et al.*, Duration of Reduction in Enduring Stress-Induced Hyperalgesia
555 Via FKBP51 Inhibition Depends on Timing of Administration Relative to Traumatic
556 Stress Exposure. *J. Pain* **23**, 1256–1267 (2022).

557 7. A. V. Bortsov, *et al.*, Polymorphisms in the glucocorticoid receptor co-chaperone FKBP5
558 predict persistent musculoskeletal pain after traumatic stress exposure. *Pain* **154**,
559 1419–1426 (2013).

560 8. S. D. Linnstaedt, *et al.*, A Functional riboSNitch in the 3' Untranslated Region of *FKBP5*
561 Alters MicroRNA-320a Binding Efficiency and Mediates Vulnerability to Chronic Post-
562 Traumatic Pain. *J. Neurosci.* **38**, 8407–8420 (2018).

563 9. J. J. Lobo, L. J. Ayoub, M. Moayedi, S. D. Linnstaedt, Hippocampal volume, FKBP5
564 genetic risk alleles, and childhood trauma interact to increase vulnerability to chronic
565 multisite musculoskeletal pain. *Sci. Rep.* **12**, 6511 (2022).

566 10. A. S. Zannas, T. Wiechmann, N. C. Gassen, E. B. Binder, Gene–Stress–Epigenetic
567 Regulation of FKBP5: Clinical and Translational Implications.
568 *Neuropsychopharmacology* **41**, 261–274 (2016).

569 11. J. Hartmann, *et al.*, Pharmacological Inhibition of the Psychiatric Risk Factor FKBP51
570 Has Anxiolytic Properties. *J. Neurosci. Off. J. Soc. Neurosci.* **35**, 9007–9016 (2015).

571 12. J. Hartmann, *et al.*, The involvement of FK506-binding protein 51 (FKBP5) in the
572 behavioral and neuroendocrine effects of chronic social defeat stress.
573 *Neuropharmacology* **62**, 332–339 (2012).

574 13. S. Albu, *et al.*, Deficiency of FK506-binding protein (FKBP) 51 alters sleep architecture
575 and recovery sleep responses to stress in mice. *J. Sleep Res.* **23**, 176–185 (2014).

576 14. S. Hestehave, *et al.*, Differences in multidimensional phenotype of 2 joint pain models
577 link early weight-bearing deficit to late depressive-like behavior in male mice. *PAIN*
578 *Rep.* **9**, e1213 (2024).

15. S. Gaali, *et al.*, Selective inhibitors of the FK506-binding protein 51 by induced fit. *Nat. Chem. Biol.* **11**, 33–37 (2015).

16. R. J. Blanchard, D. C. Blanchard, Passive and active reactions to fear-eliciting stimuli. *J. Comp. Physiol. Psychol.* **68**, 129–135 (1969).

17. G. Corder, *et al.*, Loss of μ opioid receptor signaling in nociceptors, but not microglia, abrogates morphine tolerance without disrupting analgesia. *Nat. Med.* **23**, 164–173 (2017).

18. Z. Ardi, A. Albrecht, A. Richter-Levin, R. Saha, G. Richter-Levin, Behavioral profiling as a translational approach in an animal model of posttraumatic stress disorder. *Neurobiol. Dis.* **88**, 139–147 (2016).

19. I. Sarkar, M. Snippe-Strauss, A. Tenenhaus Zamir, A. Benhos, G. Richter-Levin, Individual behavioral profiling as a translational approach to assess treatment efficacy in an animal model of post-traumatic stress disorder. *Front. Neurosci.* **16**, 1071482 (2022).

20. L. Brown, A. Fisk, C. Pothecary, S. Peirson, Telling the Time with a Broken Clock: Quantifying Circadian Disruption in Animal Models. *Biology* **8**, 18 (2019).

21. A. I. Pack, *et al.*, Novel method for high-throughput phenotyping of sleep in mice. *Physiol. Genomics* **28**, 232–238 (2007).

22. S. P. Fisher, *et al.*, Rapid Assessment of Sleep-Wake Behavior in Mice. *J. Biol. Rhythms* **27**, 48–58 (2012).

23. R. Urban, G. Scherrer, E. H. Goulding, L. H. Tecott, A. I. Basbaum, Behavioral indices of ongoing pain are largely unchanged in male mice with tissue or nerve injury-induced mechanical hypersensitivity. *Pain* **152**, 990–1000 (2011).

24. S. Wedel, *et al.*, SAFit2 ameliorates paclitaxel-induced neuropathic pain by reducing spinal gliosis and elevating pro-resolving lipid mediators. *J. Neuroinflammation* **20**, 149 (2023).

25. L. A. Stechschulte, *et al.*, FKBP51 Null Mice Are Resistant to Diet-Induced Obesity and the PPARγ Agonist Rosiglitazone. *Endocrinology* **157**, 3888–3900 (2016).

26. A. S. Häusl, *et al.*, Mediobasal hypothalamic FKBP51 acts as a molecular switch linking autophagy to whole-body metabolism. *Sci. Adv.* **8**, eabi4797 (2022).

27. C. Engelhardt, *et al.*, FKBP51 in the Oval Bed Nucleus of the Stria Terminalis Regulates Anxiety-Like Behavior. *eNeuro* **8**, ENEURO.0425-21.2021 (2021).

28. J. C. O'Leary, *et al.*, A New Anti-Depressive Strategy for the Elderly: Ablation of FKBP5/FKBP51. *PLoS ONE* **6**, e24840 (2011).

29. Q. Han, *et al.*, SHANK3 Deficiency Impairs Heat Hyperalgesia and TRPV1 Signaling in Primary Sensory Neurons. *Neuron* **92**, 1279–1293 (2016).

30. M. D. Schaffler, L. J. Middleton, I. Abdus-Saboor, Mechanisms of Tactile Sensory Phenotypes in Autism: Current Understanding and Future Directions for Research. *Curr. Psychiatry Rep.* **21** (2019).

31. Y. Fang, *et al.*, Astrocytic phosphatase and tensin homolog deleted on chromosome 10 regulates neuropathic pain by facilitating 3-hydroxy-3-methylglutaryl-CoA reductase–dependent cholesterol biosynthesis. *Pain* **163**, e1192–e1206 (2022).

32. Y. Fotio, *et al.*, NAAA-regulated lipid signaling governs the transition from acute to chronic pain. *Sci. Adv.* **7**, eabi8834 (2021).

33. A. C. Ogbonna, A. K. Clark, M. Malcangio, Development of monosodium acetate-induced osteoarthritis and inflammatory pain in ageing mice. *Age Dordr. Neth.* **37**, 9792 (2015).

34. A. C. Ogbonna, A. K. Clark, C. Gentry, C. Hobbs, M. Malcangio, Pain-like behaviour and spinal changes in the monosodium iodoacetate model of osteoarthritis in C57Bl/6 mice: Pain and spinal changes in mouse MIA model of OA. *Eur. J. Pain* **17**, 514–526 (2013).

35. T. Pitcher, J. Sousa-Valente, M. Malcangio, The Monoiodoacetate Model of Osteoarthritis Pain in the Mouse. *J. Vis. Exp.* (2016). https://doi.org/10.3791/53746.

36. M. Thakur, W. Rahman, C. Hobbs, A. H. Dickenson, D. L. H. Bennett, Characterisation of a Peripheral Neuropathic Component of the Rat Monoiodoacetate Model of Osteoarthritis. *PLoS ONE* **7**, e33730 (2012).

37. J. De Sousa Valente, The Pharmacology of Pain Associated With the Monoiodoacetate Model of Osteoarthritis. *Front. Pharmacol.* **10**, 974 (2019).

38. V. L. Harvey, A. H. Dickenson, Behavioural and electrophysiological characterisation of experimentally induced osteoarthritis and neuropathy in C57Bl/6 mice. *Mol. Pain* **5**, 18 (2009).

39. K. Kobayashi, *et al.*, Sodium iodoacetate-induced experimental osteoarthritis and associated pain model in rats. *J. Vet. Med. Sci.* **65**, 1195–1199 (2003).

40. J. Axford, *et al.*, Prevalence of anxiety and depression in osteoarthritis: use of the Hospital Anxiety and Depression Scale as a screening tool. *Clin. Rheumatol.* **29**, 1277–1283 (2010).

41. J. Sellmeijer, *et al.*, Hyperactivity of Anterior Cingulate Cortex Areas 24a/24b Drives Chronic Pain-Induced Anxiodepressive-like Consequences. *J. Neurosci. Off. J. Soc. Neurosci.* **38**, 3102–3115 (2018).

42. S. Hestehave, *et al.*, The influence of rat strain on the development of neuropathic pain and comorbid anxio-depressive behaviour after nerve injury. *Sci. Rep.* **10**, 20981 (2020).

43. I. N. Ackerman, C. Pratt, A. Gorelik, D. Liew, The projected burden of osteoarthritis and rheumatoid arthritis in Australia: A population-level analysis. *Arthritis Care Res.* (2017). https://doi.org/10.1002/acr.23414.

654 44. J. Park, A. Mendy, E. R. Vieira, Various Types of Arthritis in the United States:
655 Prevalence and Age-Related Trends From 1999 to 2014. *Am. J. Public Health* e1–e3
656 (2017). https://doi.org/10.2105/AJPH.2017.304179.

657 45. A. Sharma, P. Kudesia, Q. Shi, R. Gandhi, Anxiety and depression in patients with
658 osteoarthritis: impact and management challenges. *Open Access Rheumatol. Res. Rev.*
659 **Volume 8**, 103–113 (2016).

660 46. E. L. Dimitrov, M. C. Tsuda, H. A. Cameron, T. B. Usdin, Anxiety- and depression-like
661 behavior and impaired neurogenesis evoked by peripheral neuropathy persist
662 following resolution of prolonged tactile hypersensitivity. *J. Neurosci. Off. J. Soc.*
663 *Neurosci.* **34**, 12304–12312 (2014).

664 47. M. G. Codagnone, *et al.*, Inhibition of FKBP51 induces stress resilience and alters
665 hippocampal neurogenesis. *Mol. Psychiatry* **27**, 4928–4938 (2022).

666 48. A. Hähle, S. Merz, C. Meyners, F. Hausch, The Many Faces of FKBP51. *Biomolecules* **9**,
667 35 (2019).

668 49. X. Ma, R. Peterson, J. Turnbull, Adenylyl Cyclase type 3, a marker of primary cilia, is
669 reduced in primary cell culture and in lumbar spinal cord in situ in G93A SOD1 mice.
670 *BMC Neurosci.* **12** (2011).

671 50. K. Tucker, *et al.*, The Primary Cilium and its Hedgehog Signaling in
672 NociceptorsContribute to Inflammatory and Neuropathic Pain. [Preprint] (2024).
673 Available at: https://www.researchsquare.com/article/rs-3812442/v1 [Accessed 17
674 September 2024].

675 51. R. R. Fagan, *et al.*, Selective targeting of mu opioid receptors to primary cilia. *Cell Rep.*
676 **43**, 114164 (2024).

677 52. W. M. Walwyn, *et al.*, Sustained Suppression of Hyperalgesia during Latent
678 Sensitization by μ-, δ-, and κ-opioid receptors and α_{2A} Adrenergic Receptors: Role of
679 Constitutive Activity. *J. Neurosci.* **36**, 204–221 (2016).

680 53. V. Buffa, *et al.*, Analysis of the Selective Antagonist SAFit2 as a Chemical Probe for the
681 FK506-Binding Protein 51. *ACS Pharmacol. Transl. Sci.* **6**, 361–371 (2023).

682 54. W. J. Dixon, Efficient Analysis of Experimental Observations. *Annu. Rev. Pharmacol.*
683 *Toxicol.* **20**, 441–462 (1980).

684 55. A. E. Learoyd, D. Sen, M. Fitzgerald, The pain trajectory of juvenile idiopathic arthritis
685 (JIA): translating from adolescent patient report to behavioural sensitivity in a juvenile
686 animal model. *Pediatr. Rheumatol.* **17**, 60 (2019).

687 56. K. Ängeby Möller, C. Aulin, A. Baharpoor, C. I. Svensson, Pain behaviour assessments by
688 gait and weight bearing in surgically induced osteoarthritis and inflammatory arthritis.
689 *Physiol. Behav.* **225**, 113079 (2020).

690 57. C. Mills, *et al.*, Estimating Efficacy and Drug ED50's Using von Frey Thresholds: Impact
691 of Weber's Law and Log Transformation. *J. Pain* **13**, 519–523 (2012).

692

Figures and legends

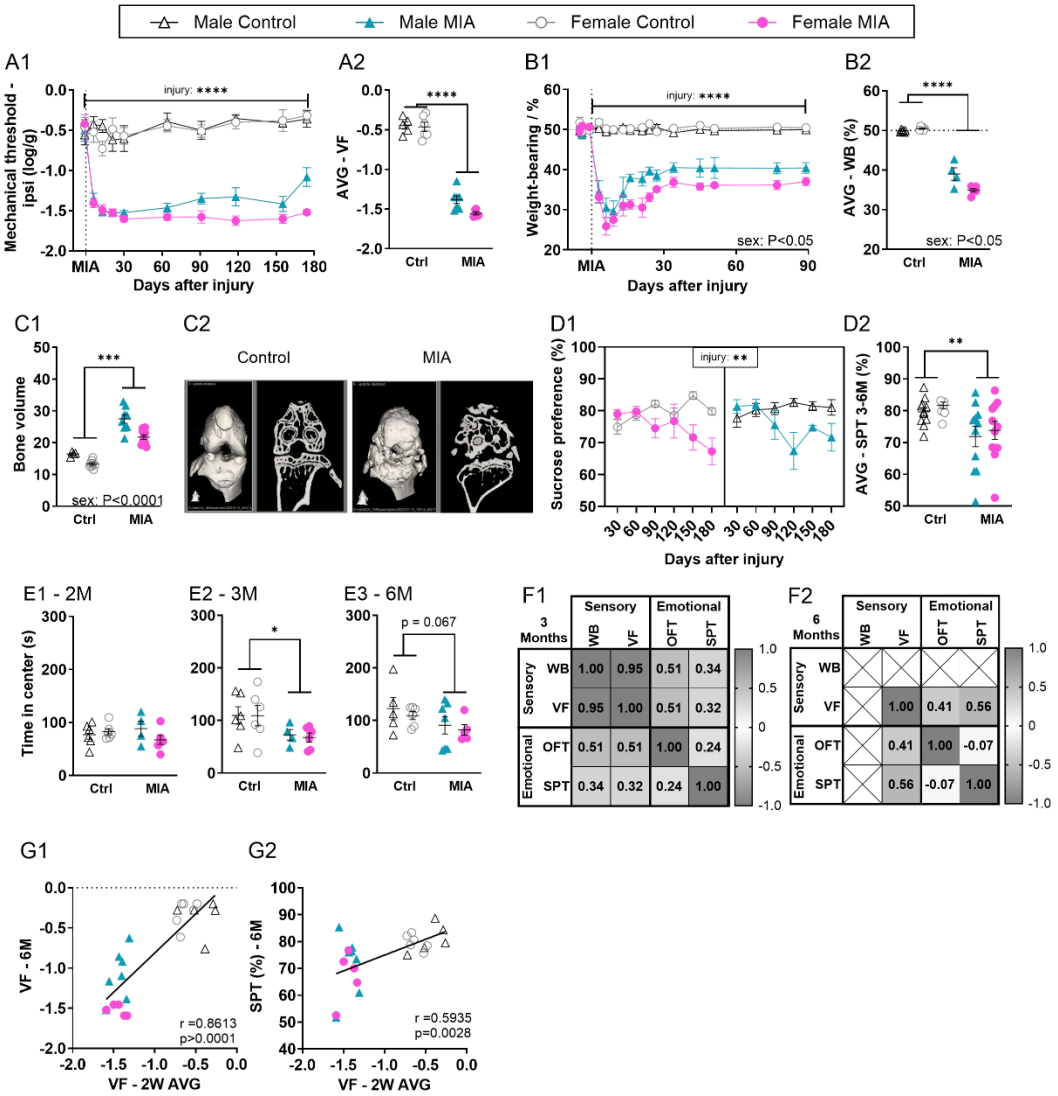

Figure 1: MIA induces immediate and persistent sensory and functional changes, but delayed anxio-depressive comorbidities. (A1,2) Mechanical hypersensitivity assessed using von Frey (vF) filaments (N=5-7). **(B1,2)** Functional deficit assessed using static weight bearing (WB) distribution (N=4-6). **(C1,2)** Bone volume around the joint, assessed using microCT at 6 months after injury (N=4-11). C2: Typical micro-CT image of control and MIA female joint. **(D1,2)** Depressive-like behaviour (anhedonia) assessed using the Sucrose Preference Test (two bottle test, water vs 1% sucrose). Data shows % consumption of the sucrose water compared with pure water. Weighted average (AVG) in D2 was calculated from 3-6months data. (N=4-12). **(E1,2,3)** Anxiety-like behaviour assessed using the Open Field Test measured at 2 (E1), 3 (E2) and 6 (E3) months after injury (N=4-7). **(F1,2)** Correlations between outcomes recorded from the same animal at the same time point at 3 (F1) and 6 (F2) months (N=22-23 across groups). **(G1,2)** Correlations between early-stage mechanical sensitivity (2-week weighted average) and the later stage (6 months) hypersensitivity (G1) and depressive-like (G2) behaviour. **A2, B2**: Weighted average (AVG) calculated across the full study period. Data shows mean ± S.E.M. NS= Not significant, *P<0.05, **P<0.01, ***P<0.001, ****P<0.0001, as determined by ANOVA-analysis. See full statistical analysis in SI Appendix Table S2.

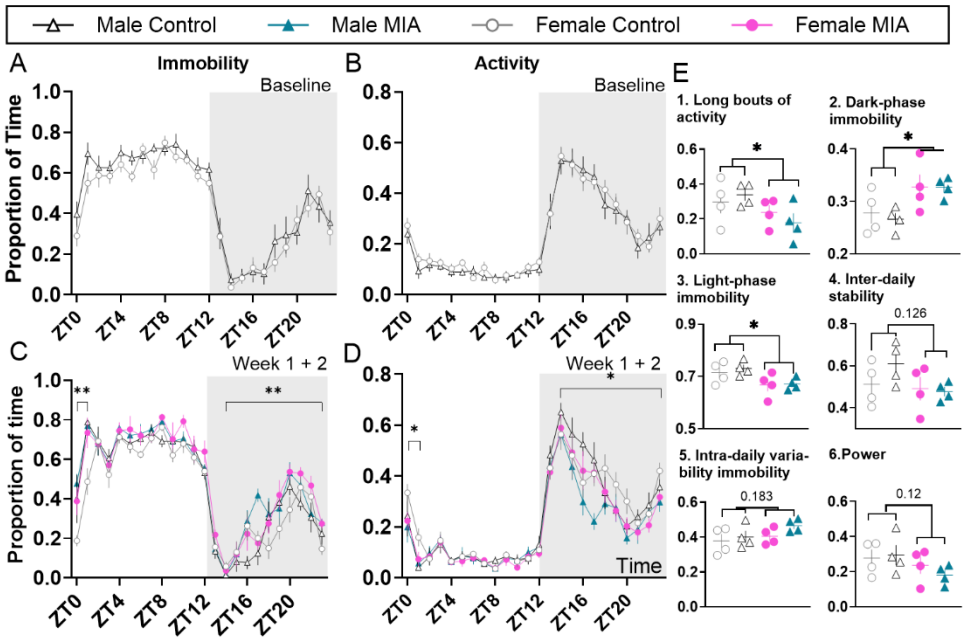

Figure 2: MIA-induced joint pain is accompanied by fragmented daily activity rhythms in the first 2 weeks. (A-D) 24h immobility/activity plots using 1h bins. **(A, B)** Average of 24h plots across the 6 days before MIA injection. N=8. **(C, D)** Average of 24h plots across the first 2 weeks after MIA injection. N=4. **(E) (E1)** proportion of time spent in long bouts (>10min) activity during the dark period, **(E2)** proportion of time spent in immobility during the dark phase, **(E3)** proportion of time spent immobile during the light phase, **(E4)** interdaily stability as a stability index, with higher values representing highly stable patterns, **(E5)**, intra-daily variability immobility as a variability index, with higher values representing highly fragmented patterns and **(E6)** strength of the rhythmicity; power of the 24-hour activity cycle calculated across 2 weeks. The power of a periodogram provides a measure of the strength and regularity of the underlying rhythm, with higher values indicating robust rhythms. In circadian disruption—where rhythms are typically less robust—the power is expected to be reduced, which may indicate the absence of a significant circadian rhythm. N=4. ZT0=7am, ZT12=7pm. Data shows mean ± S.E.M. *P<0.05; ** P<0.01, injury effect. See full statistical analysis in SI Appendix Table S2.

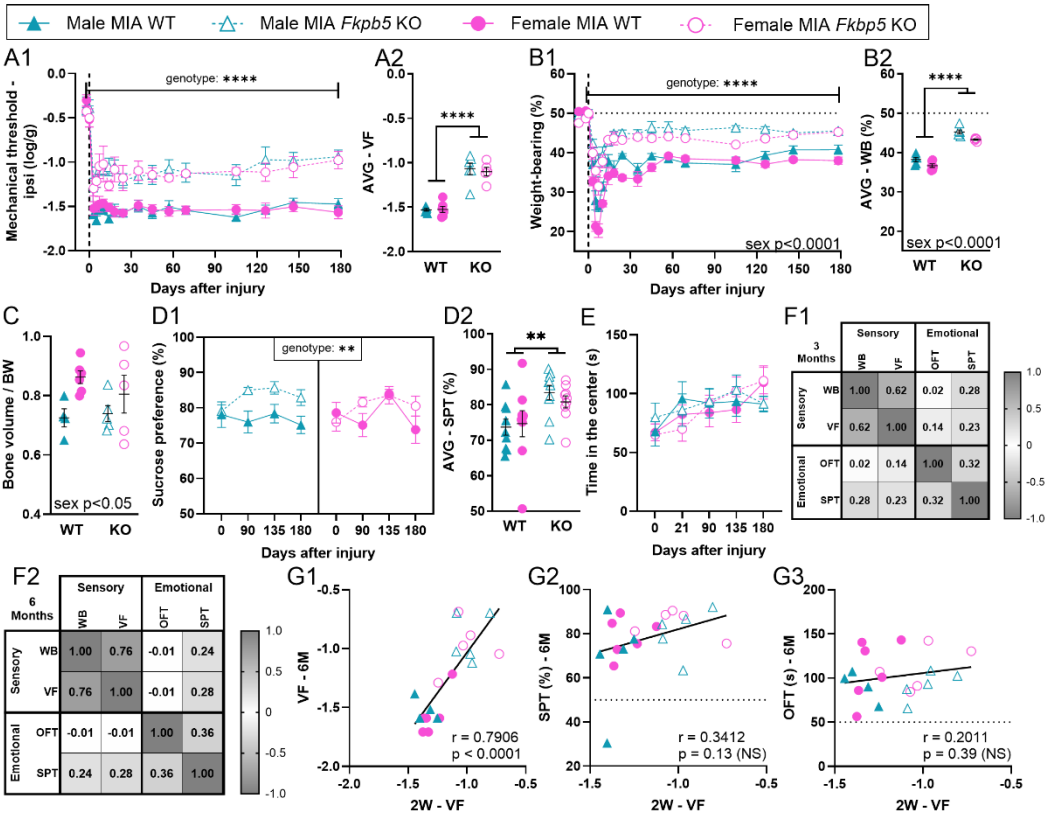

Figure 3: *Fkbp5* global knock-out improves sensory, functional and depressive-like behaviour induced by MIA. (A1,2) Mechanical hypersensitivity assessed using von Frey filaments (N=5-6). **(B1,2)** Functional deficits assessed using static weight bearing distribution (N=5-6). **(C)** Bone volume around the joint assessed by microCT at 6 months after injury and normalised to body weight (N=4-6). **(D1,2)** Depressive-like behaviour (anhedonia) assessed using the Sucrose Preference Test (two-bottle test, water vs 1% sucrose). Data shows % consumption of the sucrose water compared with pure water. Weighted average (AVG) in D2 was calculated from 3-6months data. (N=5-9). **(E)** Anxiety-like behaviour assessed using the Open Field Test (N=5-6). **(F1,2)** Correlations between outcomes recorded from the same animal at the same time point at 3 (F1) and 6 (F2) months (N=22 across groups). **(G1,2,3)** Correlations between early-stage mechanical sensitivity (2-week weighted average) and the later stage (6 months) of hypersensitivity (G1), depressive-like (G2) and anxiety-like (G3) behaviour. **A2, B2**: Weighted average (AVG) calculated across the full study period. Data shows mean ± S.E.M. *P<0.05, **P<0.01, ***P<0.001, ****P<0.0001, as determined by ANOVA analysis. See full statistical analysis in SI Appendix Table S2.

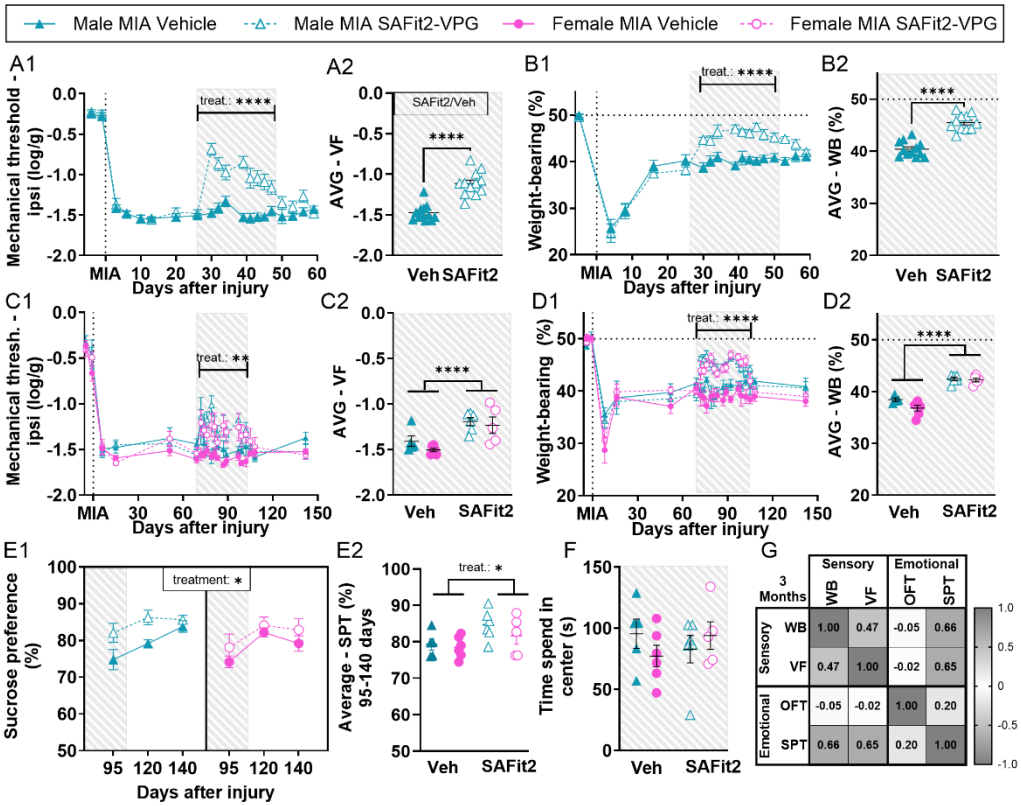

Figure 4: Pharmacological inhibition of FKBP51 after MIA induction transiently improves sensory and functional deficits and delays the onset of depressive-like behaviors. Hatched grey area indicates when SAFit2 was active. (**A1,2**) Mechanical hypersensitivity assessed in male mice using von Frey filaments. (N=12). (**B1,2**) Functional deficits assessed using static weight bearing distribution (N=11-12). (**C1,2**) Mechanical hypersensitivity assessed using von Frey filaments. SAFit2-VPG was administered 10-14 weeks after injury. (N=5-6). (**D1,2**) Functional deficits assessed using static weight bearing distribution. (N=4-6). (**E1,2**) Depressive-like behaviour (anhedonia) assessed using the Sucrose Preference Test (two-bottle test, water vs 1% sucrose). Data shows % consumption of the sucrose water compared with pure water. Weighted average in E2 was calculated from D95-140 data (N=5-6). (**F**) Anxiety-like behaviour assessed using the Open Field Test (N=5-6). (**G**) Correlations between outcomes recorded from the same animal at the same time point at 3 months after injury (14 weeks), when SAFit2-VPG was administered from 10-14 weeks after injury (N=21 across groups). A2, B2, C2, D2: Weighted average (AVG) was calculated for the hatched grey study period, where the compound was active. Data shows mean ± S.E.M. *P<0.05, **P<0.01, ***P<0.001, ****P<0.0001, as determined using ANOVA analysis. See full statistical analysis in SI Appendix Table S2.

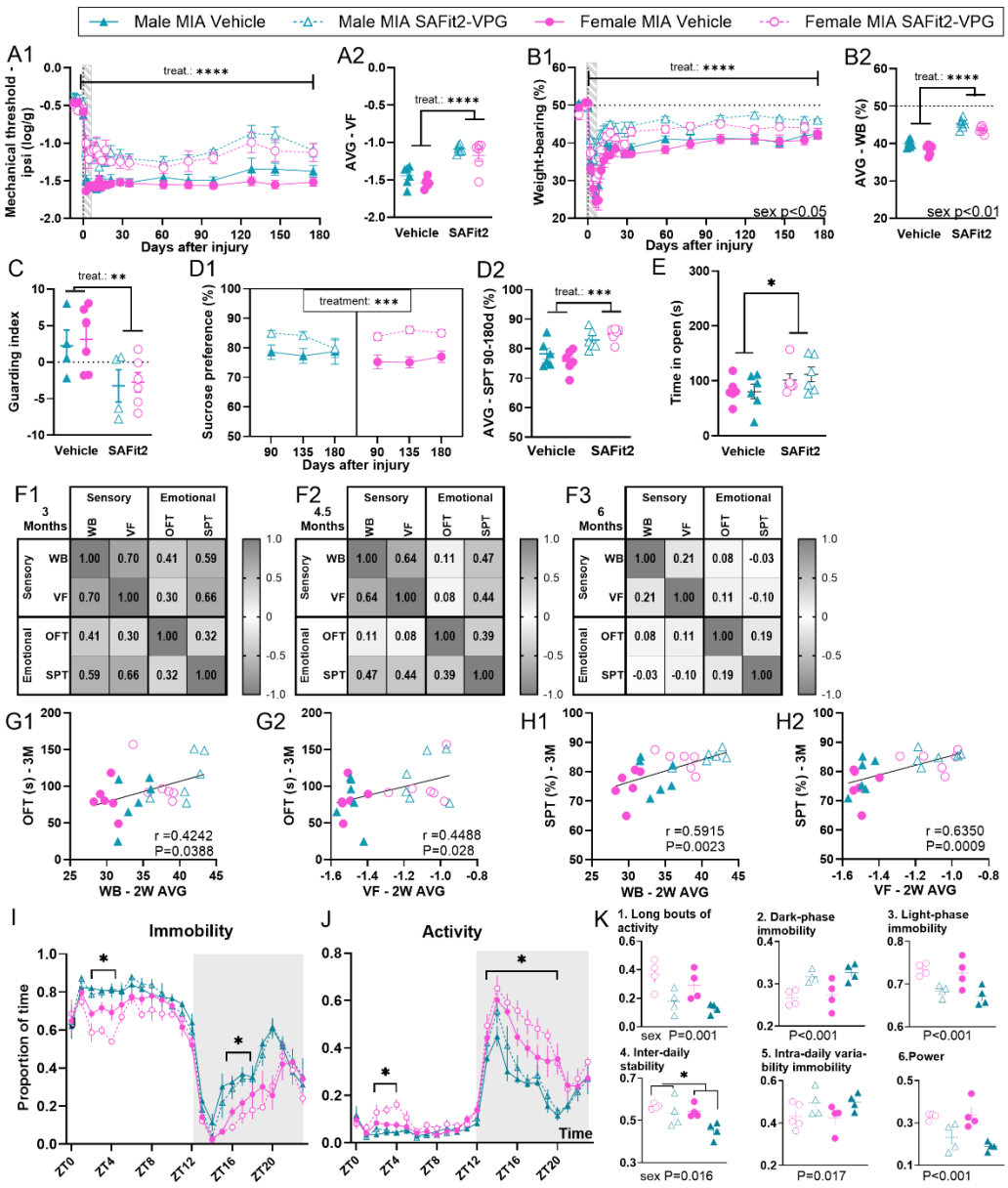

Figure 5: Acute pharmacological inhibition of FKBP51 initiated during joint pain onset prevents the full development of MIA-induced symptoms. SAFit2-VPG was injected 3 days before MIA. Hatched grey area indicates when SAFit2 was active. (**A1,2**) Mechanical hypersensitivity assessed using von Frey filaments (N=6). (**B1,2**) Functional deficits assessed using static weight bearing distribution (N=6). (**C**) Guarding index at 6 weeks after injury, 4 weeks after SAFit2 was active, assessed by Catwalk gait analysis (N=4-6). (**D1,2**) Depressive-like behaviour (anhedonia) assessed using the Sucrose Preference Test (two-bottle test, water vs 1% sucrose). Data shows % consumption of the sucrose water compared with pure water. Weighted average (AVG) in D2 was calculated from 3-6months data (N=6). (**E**) Anxiety-like behaviour assessed using the Open Field Test (N=6). (**F1,2,3**) Correlations between outcomes recorded **from** the same animal at 3 (**F1**), 4.5 (**F2**) and 6 (**F3**) months after injury (N=6). (**G, H**) Correlations between the weighted average weight bearing asymmetry (WB) or mechanical hypersensitivity (vF) from the first two weeks after injury, when the compound was active, and the level of anxiety-like behaviour at 3 months (**G1,2**), and the level of depressive-like behaviour at 3 months (**H1,2**). **(I, J)** 24h immobility/activity plots using 1h bins across the first 2 weeks after MIA injection. N=4. **(K)** Average across 14 days after MIA. **(K1)** Proportion of time spent in long bouts (>10min) activity during the dark period, **(K2)** proportion of time spent immobile during the dark phase, **(K3)** proportion of time spent immobile during the light phase, **(K4)**

interdaily stability as a stability index, with higher values representing highly stable patterns, **(K5)** intra-daily variability immobility as a variability index, with higher values representing highly fragmented patterns and **(K6)** strength of the rhythmicity; power of the 24-hour activity cycle calculated across 2 weeks. A2, B2: Weighted average (AVG) was calculated for the full study period. Data shows mean ± S.E.M. *P<0.05, **P<0.01, ***P<0.001, ****P<0.0001, as determined using ANOVA-analysis. Full statistical analysis in SI Appendix Table S2.

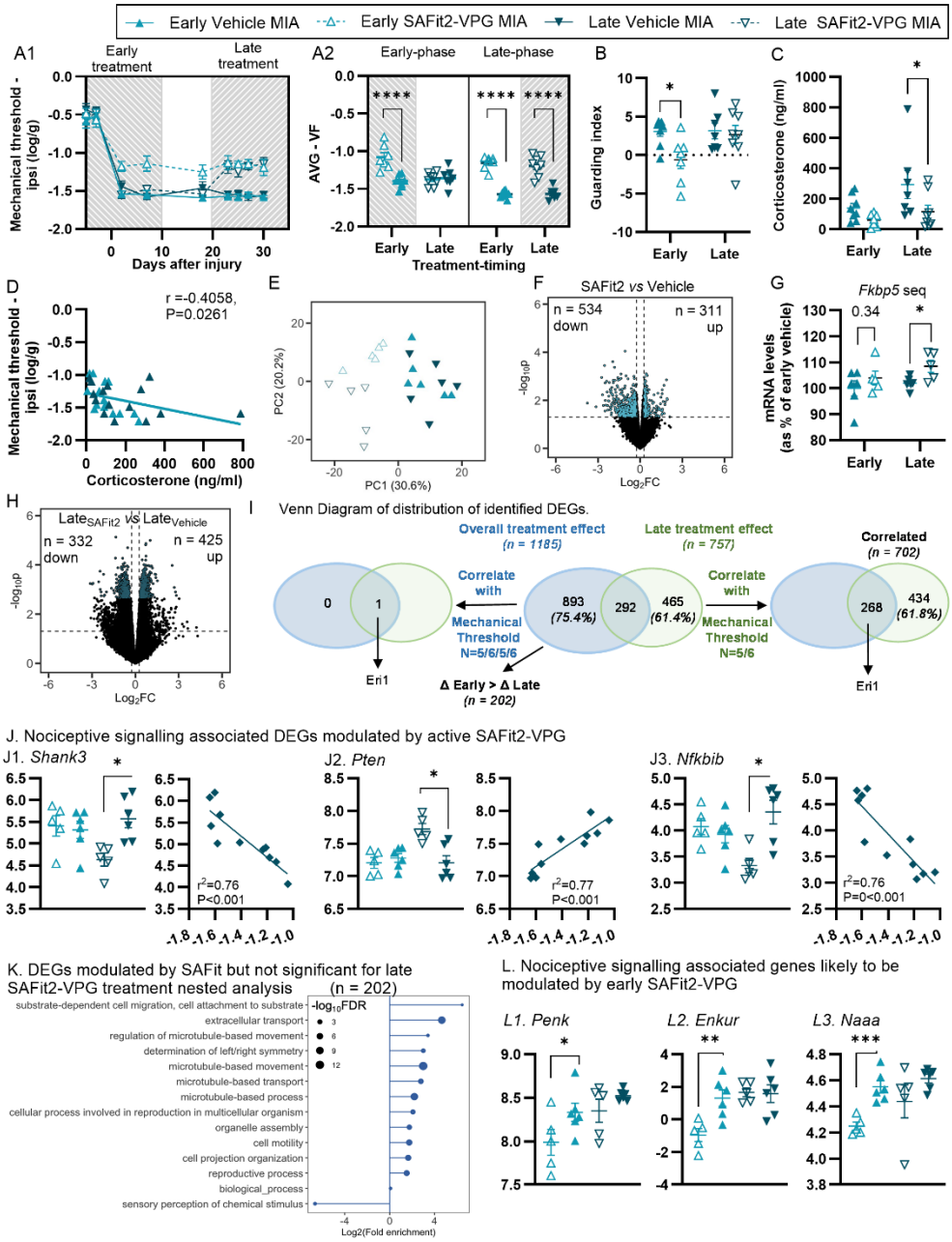

Figure 6: Pharmacological inhibition of FKBP51 initiated either before or after pain state induction leads to different gene expression changes. SAFit2-VPG was injected either "Early" (day –3 and day 4), or "Late" (day 20 and day 27). Hatched grey area indicates the active phase of SAFit2. (**A1,2**) Mechanical hypersensitivity assessed using von Frey filaments. **A1**: Data shows Mean ± S.E.M. (**B**) Guarding index assessed through catwalk gait analysis. (**C**) Corticosterone levels (Day 31). (**D**) Correlation between mechanical allodynia and corticosterone (Day 31). (**E**) PCA Analysis indicating sub-clusters within the second principal component of SAFit2-treated groups not present in vehicle-treated groups. (**F**) Volcano plots; x-axis: log2-transformed fold change in gene expression between SAFit2 and vehicle treated groups. (**G**) Expression levels of *Fkbp5* mRNA from sequencing counts. (**H**) Volcano plots; x-

axis: log2-transformed fold change in gene expression between $Late_{SAFit2}$ and $Late_{vehicle}$ treated groups; (**I**) Venn Diagram of distribution of identified DEGs. **(J)** DEGs by SAFit2-VPG late treatment associated with nociceptive signalling. *P<0.05, as per nested analysis; correlation graphs show the results of Pearson Correlation analysis. y-axis: log_2CPM, x-axis: mechanical thresholds (log(G)). (**K**) Lollipop plot of enriched Gene Ontology (GO) terms identified by PANTHER from the differentially expressed genes (DEGs) between SAFit2 and vehicle treated mice;,emphasis on genes with a greater change in expression between ($Early_{SAFit2}$ vs $Early_{Vehicle}$) than ($Late_{SAFit2}$ vs $Late_{Vehicle}$). The X-axis represents the GO terms related to biological processes while the Y-axis shows the fold change in enrichment. Significance (-log10 adjusted P-value) of each term is denoted by size. (**L**) Selected genes associated with nociceptive signalling. Y-axis: log_2CPM. (**F,H**): y-axis represents the –log10(p-value) for differential expression; coloured points are significantly up- or down-regulated with threshold abs(log2FC) >1.2; vertical dotted lines represent log2FC thresholds: left: log2FC=-1 (2-fold downregulation) and right: log2FC=1 (2 fold upregulation); horizontal dotted line represents the p-value threshold. *P<0.05; **P<0.01; ***P<0.001, t-test $Early_{SAFit2}$ vs $Early_{Vehicle.}$ For all graphs; (N=7-8), See full statistical analysis in SI Appendix Table S2.